Supplementary Material (ESI) for Chemical Communications


*Supporting Information*

# Two spin-competing manganese coordination polymers exhibiting unusual multi-step magnetization jumps

**Wei-Xiong Zhang, Wei Xue, Yan-Zhen Zheng and Xiao-Ming Chen***

MOE Key Laboratory of Bioinorganic and Synthetic Chemistry, School of Chemistry and Chemical Engineering, Sun Yat-Sen University, Guangzhou 510275, China.

Fax: +86-20-84112245; Tel: +86-20-84112074

e-mail: cxm@mail.sysu.edu.cn

## *Preparation*

1,2,3-Triazole-4,5-dicarboxylic acid ($H_3$tzdc) was synthesized according to the patent method.[1] $MnCO_3$ was synthesised by $MnCl_2{\cdot}6H_2O$ and $Na_2CO_3$. All other reagents and solvents employed were commercially available and used as received without further purification. The C, H and N elemental analyses were carried out with a Vario EL elemental analyzer.

**Preparation of $Mn_3(tzdc)_2(H_2O)_2(NH_3)_2$ (1)**: A mixture of $MnCl_2{\cdot}6H_2O$ (0.119 g, 0.6 mmol), $H_3$tzdc$\cdot 2H_2O$ (0.077 g, 0.4 mmol), $H_2O$ (1 mL), ethanol (1 mL) and aqueous ammonia (1.0 mL) was sealed in a 6-mL Teflon-lined stainless autoclave and heated at 140 °C for 3 days, followed by slow cooling (0.1 $^{o}$C/min) to room temperature. The precipitate was washed by ultrasonic cleaning and then the colourless crystals of **1** were collected in a yield of 20% based on $H_3$tzdc$\cdot 2H_2O$. Elemental analysis calc. for $C_8H_{10}Mn_3N_8O_{10}$: C, 17.69; H, 1.86; N, 20.64%; found: C, 17.73; H, 1.92; N, 20.78%.

**Preparation of $Mn_3(tzdc)_2(H_2O)_4$ (2):** A mixture of freshly prepared $MnCO_3$ (0.115 g, 1.0 mmol), $H_3$tzdc$\cdot 2H_2O$ (0.192 g, 1.0 mmol) and $H_2O$ (10 mL) was sealed in a 23-mL Teflon-lined stainless autoclave and heated at 160 °C for 3 days, followed by slow cooling (0.1 $^{o}$C/min) to room temperature. The colourless block crystals of **2** were collected in a yield of 70% based on $MnCO_3$. Elemental analysis calc. for $C_8H_8Mn_3N_6O_{12}$: C, 17.63; H, 1.48; N, 15.42%; found: C, 17.64; H, 1.53; N, 15.21%.

**The single-crystal X-ray crystallography**: The diffraction intensities were collected at 298(2) K on a Bruker Apex CCD area-detector diffractometer (Mo$K_\alpha$, $\lambda$ = 0.71073 Å). All

intensity data were corrected for Lorentz and polarization effects, and empirical absorption corrections based on equivalent reflections were applied (SADABS). The structures were solved by direct methods and refined by the full-matrix least-squares method on $F^2$ with SHELXTL program package.[2] All non-hydrogen atoms were refined with anisotropic displacement parameters. The H atoms were generated geometrically. Selected bond distances and bond angles are listed in Table S1.

In the structure of **2**, there is a pseudo symmetry element (Checkcif report, Alert B), it should be mainly caused by the $\mu_5$-tzdc$^{3-}$-bridged chain running along the b axis (Fig. 2b), which has a local inversion centre between Mn1 and Mn2 atoms.

Crystal data for **1**: $C_8H_{10}Mn_3N_8O_{10}$, $M$ = 543.06, monoclinic, space group $P2_1/c$, $T$ =298(2) K, $a$ = 12.293(1), $b$ = 9.453(1), $c$ = 7.296(1) Å, $\beta$ = 99.465(2)°, $V$ = 836.3(2) Å$^3$, $Z$ = 2, $D_c$ = 2.157 g·cm$^{-3}$, $\mu$ = 2.305 mm$^{-1}$, a total of 4014 reflections were collected, 1623 of which were unique ($R_{int}$ = 0.02), final $R_1$ = 0.0364 for $I > 2\sigma(I)$, $wR_2$ = 0.0912 for all data, GOF = 1.047, CCDC 724458;

Crystal data For **2**: $C_8H_8Mn_3N_6O_{12}$, $M$ = 545.02, monoclinic, space group $P2_1/c$, $T$ =298(2) K, $a$ = 7.560(1), $b$ = 16.358(1), $c$ = 13.073(1) Å, $\beta$ = 92.652(1)°, $V$ = 1615.0(2) Å$^3$, $Z$ = 4, $D_c$ = 2.242 g·cm$^{-3}$, $\mu$ = 2.394 mm$^{-1}$, a total of 6982 reflections were collected, 3087 of which were unique ($R_{int}$ = 0.0172), final $R_1$ = 0.03 for $I > 2\sigma(I)$, $wR_2$ = 0.0784 for all data, GOF = 1.071, CCDC 724459.

[1] G. H. Suverkropp, P. L. Alsters, C. S. Snijder and J. G. De Vries, *US Pat*., 5 917 049, 1999;
[2] *SHELXTL 6.10*, Bruker Analytical Instrumentation, Madison, Wisconsin, USA, 2000.

Table S1 Selected bond lengths (Å) and bond angles (°) for **1** and **2**

| | | | | | |
|---|---|---|---|---|---|
| **1**[a] | | | | | |
| Mn1-O1 | 2.195(2) | O1-Mn1-N4 | 91.1(1) | O1W-Mn2-O4C | 87.90(9) |
| Mn1-N1 | 2.262(2) | N1-Mn1-N4 | 94.6(1) | O2-Mn2-O3 | 84.94(8) |
| Mn1-N4 | 2.263(3) | O1-Mn1-N1A | 106.02(8) | O3B-Mn2-O3 | 74.28(8) |
| Mn2-O2 | 2.107(2) | O1-Mn1-N4A | 88.9(1) | O1W-Mn2-O3 | 164.95(9) |
| Mn2-O3B | 2.168(2) | N1A-Mn1-N4 | 85.4(1) | O4C-Mn2-O3 | 83.85(8) |
| Mn2-O1W | 2.185(3) | O2-Mn2-O3B | 98.04(9) | O2-Mn2-N3C | 91.87(9) |
| Mn2-O4C | 2.225(2) | O2-Mn2-O1W | 106.17(9) | O3B-Mn2-N3C | 162.57(8) |
| Mn2-O3 | 2.243(2) | O3B-Mn2-O1W | 93.80(9) | O1W-Mn2-N3C | 97.2(1) |
| Mn2-N3C | 2.258(2) | O2-Mn2-O4C | 160.91(8) | O4C-Mn2-N3C | 73.27(8) |
| O1-Mn1-N1 | 73.98(8) | O3B-Mn2-O4C | 93.73(8) | O3-Mn2-N3C | 92.47(8) |
| **2**[b] | | | | | |
| Mn1-N1 | 2.169(2) | O1W-Mn1-N1 | 101.41(7) | N3A-Mn2-O6 | 89.54(7) |
| Mn1-O1 | 2.314(2) | O2W-Mn1-N1 | 92.82(7) | O7-Mn2-O4A | 163.94(6) |
| Mn1-O4A | 2.167(2) | O4A-Mn1-N1 | 148.71(6) | O1-Mn2-O4A | 77.52(6) |
| Mn1-O1W | 2.098(2) | O1W-Mn1-O3W | 93.31(8) | O4W-Mn2-O4A | 88.83(6) |
| Mn1-O2W | 2.147(2) | O2W-Mn1-O3W | 168.94(7) | N3A-Mn2-O4A | 71.86(6) |
| Mn1-O3W | 2.308(2) | O4A-Mn1-O3W | 86.60(6) | O6-Mn2-O4A | 84.33(6) |
| Mn2-O1 | 2.146(2) | N1-Mn1-O3W | 80.66(7) | O2B-Mn3-O5C | 165.59(6) |
| Mn2-O6 | 2.180(2) | O1W-Mn1-O1 | 171.49(7) | O2B-Mn3-N6 | 97.38(7) |
| Mn2-O7 | 2.135(2) | O2W-Mn1-O1 | 88.88(7) | O5C-Mn3-N6 | 94.88(7) |
| Mn2-O4A | 2.353(2) | O4A-Mn1-O1 | 77.96(6) | O2B-Mn3-O3B | 85.75(7) |
| Mn2-N3A | 2.177(2) | N1-Mn1-O1 | 71.85(6) | O5C-Mn3-O3B | 84.62(7) |
| Mn2-O4W | 2.156(2) | O3W-Mn1-O1 | 80.62(6) | N6-Mn3-O3B | 100.39(6) |
| Mn3-O2B | 2.168(2) | O7-Mn2-O1 | 117.11(6) | O2B-Mn3-O8 | 86.42(6) |
| Mn3-O5C | 2.187(2) | O7-Mn2-O4W | 98.93(7) | O5C-Mn3-O8 | 104.23(7) |
| Mn3-N6 | 2.193(2) | O1-Mn2-O4W | 83.89(6) | N6-Mn3-O8 | 74.24(6) |
| Mn3-O3B | 2.203(2) | O7-Mn2-N3A | 94.60(7) | O3B-Mn3-O8 | 169.85(6) |
| Mn3-O8 | 2.209(2) | O1-Mn2-N3A | 147.75(6) | O2B-Mn3-N4C | 94.88(6) |
| Mn3-N4C | 2.224(2) | O4W-Mn2-N3A | 85.59(7) | O5C-Mn3-N4C | 74.52(6) |
| O1W-Mn1-O2W | 96.75(8) | O7-Mn2-O6 | 87.03(6) | N6-Mn3-N4C | 164.15(8) |
| O1W-Mn1-O4A | 107.79(7) | O1-Mn2-O6 | 97.39(6) | O3B-Mn3-N4C | 90.46(7) |
| O2W-Mn1-O4A | 94.65(7) | O4W-Mn2-O6 | 172.58(6) | O8-Mn3-N4C | 96.63(7) |

[a]Symmetry codes for **1**: A) -x+2,-y+1,-z; B) -x+3,-y+1,-z+1; C) x,-y+3/2,z+1/2;

[b]Symmetry codes for **2**: A) -x,y+1/2,-z+3/2; B) -x+1,-y+1,-z+1; C) x,-y+3/2,z-1/2.

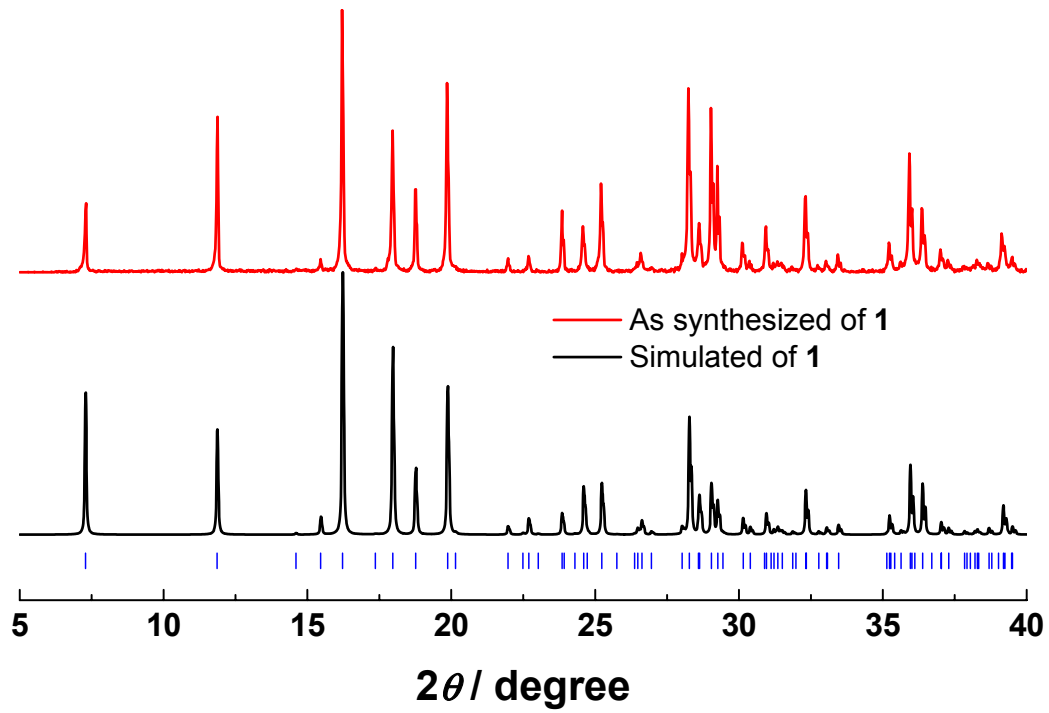


**Fig. S1** The X-ray powder diffraction patterns of **1**.

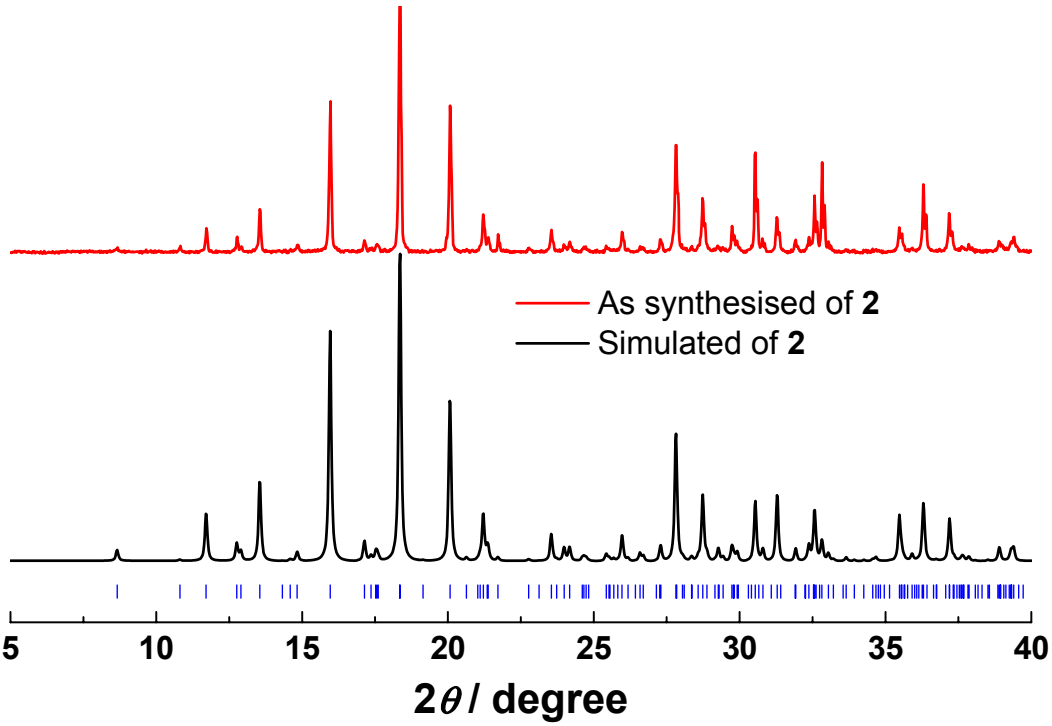


**Fig. S2** The X-ray powder diffraction patterns of **2**.

## The fitting of temperature-dependent magnetic susceptibilities of 1 and 2

Obviously, an exact theoretical treatment of magnetic properties for such complicated 3D systems cannot be carried out because there are too many kinds of magnetic exchange paths. However, the magnetic coupling interactions passed by the double $\mu_2$-O bridges should be much stronger than the other interactions passed by the single carboxylate or triazolate bridges. So we could estimate the magnetic coupling interactions, by assuming that the total magnetic susceptibility $\chi_{tol}$ is given by the sum of the single $Mn^{2+}$ ions and $Mn^{2+}$ dimers with intra-dimer ($J_1$) and inter-dimer coupling ($zJ'$).

$$\chi_{tol} = \chi_{Mn1} + \chi_{dimer} \quad (1)$$

$$\chi_{Mn1} = \frac{N\beta^2 g^2}{3kT} S(S+1) \quad (2)$$

$$\chi_{dimer} = \chi'_{dimer} / [1 - 2zJ' \chi'_{dimer} / N\beta^2 g^2] \quad (3)$$

$$\chi'_{dimer} = \frac{2N\beta^2 g^2}{kT} \cdot \frac{e^{2x} + 5e^{6x} + 14e^{12x} + 30e^{20x} + 55e^{30x}}{1 + 3e^{2x} + 5e^{6x} + 7e^{12x} + 9e^{20x} + 11e^{30x}} \quad (4)$$

Where $x$ (= $J_1/kT$) and $S$ (= 5/2) represent the spin momentum quantum number of $Mn^{2+}$, $N$ is Avogadro number, $\beta$ is the Bohr magneton, $g$ is Zeeman factor, and $k$ is Boltzmann constant. To avoid deviation of eq. (1) at low temperature because of the interaction between single ions and dimers, the data only above 20 K were fitted by least-squares method, leading to the following parameters for **1**: $g$ = 2.08(1), $J_1$ = -1.69(4) $cm^{-1}$, $zJ'$ = -0.11(4) $cm^{-1}$, $R = 3.3\times10^{-6}$; and for **2**: $g$ = 2.023(1), $J_1$ = -1.63(2) $cm^{-1}$, $zJ'$ = -0.57(3) $cm^{-1}$; $R = 2.5\times10^{-6}$ ($R = [\Sigma(\chi_{obs}T - \chi_{calc}T)^2 / \Sigma(\chi_{obs}T)^2]$).

Both of their $g$ factors are slightly larger then 2.0, which should be ascribed to certain distortions of the coordination enviroment of $Mn^{2+}$ ions (see table S1). Their $J_1$ parameters are very similar, which is consistent with the very similar bond parameters of dimers in both compounds (see Table S2). The interactions between the dimers and single ions were omitted in this model, but actually these interactions have similar amplitudes with the inter-dimer couplings. Thus, the $zJ'$ would be over-estimated in fitting due to the mixing of all these interactions. Since there are more carboxylate bridges linking the dimers and single ions in **2** than that in **1**, and some of them may passed stronger magnetic exchange interaction due to the shorter Mn···Mn distances (Table S2), which are responsible to the larger amplitude of $zJ'$ in **2**, as well as the higher citical temperature of **2**.

**Table S2** Selected bond parameters related to the magnetic exchange interactions for **1** and **2**

| Compound | | **1** | **2** |
|---|---|---|---|
| Intra-dimer | $d_{Mn\text{-}O}$ (Å) | 2.168(2), 2.243(2) | 2.146(2), 2.167(2), 2.314(2), 2.353(2) |
| | ∠Mn-O-Mn (°) | 105.73(1) | 101.30(6), 103.22(6) |
| | $d_{Mn\cdots Mn}$ (Å) | 3.517(1) | 3.497(1) |
| | $J_1$ /cm$^{-1}$ | -1.60(4) | -1.63(2) |
| The other bridges | The Mn···Mn distance bridged by carboxylate (Å) | 5.705(1), 5.949(1), 5.977(1) | 5.387(1), 5.537(1), 5.885(1), 6.015(1), 6.053(1), 6.068(1) |
| | The Mn···Mn distance bridged by triazolate (Å) | 6.641(1) | 6.400(1), 6.537(1) |
| $zJ'$/cm$^{-1}$ | | -0.24(4) | -0.57(3) |
| Weiss constant $\theta$/ K | | -11.9(2) | -15.02(5) |

## The magnetic properties measurement

The purity of powder sample was verified by powder XRD pattern collected on Bruker D8-Adavance (Figure S1, S2); The magnetic measurements were performed on a Quantum Design MPMS-XL7 SQUID magnetometer. All experimental magnetic data were corrected for the contribution of sample holder and the diamagnetic contribution calculated from Pascal constants.

The single-crystals of *ca*. 30 μg (**1**) and 40 μg (**2**) were used to perform the magnetzation measurements at 1.8 K. The relation between the crystallographic axes and single-crystal's shape was estabished after determining the orientation matrix on an Oxford CCD area-detector diffractometer. Then the single-crystal was carefully stuck on a copper wire with certain orientation by GE7031 varnish and settled on the sample holder. The magnetic field is parallel with the copper wire. The orientation accuracy of axes was estimated to be several degrees during the magnetic measurements. The magnetization data of single-crystals were corrected by comparing with the data of the powder sample, and their derivatives were smoothed.

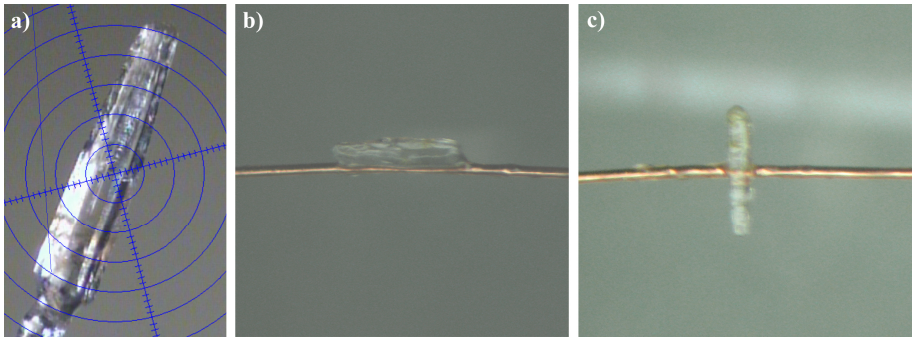


**Fig. S3** The orientated-single-crystal sample of **1** used in the magnetization measurement: a) the photo on the diffractometer; b, c) the *c* axis is parallel and perpendicular to the copper wire, respectively.

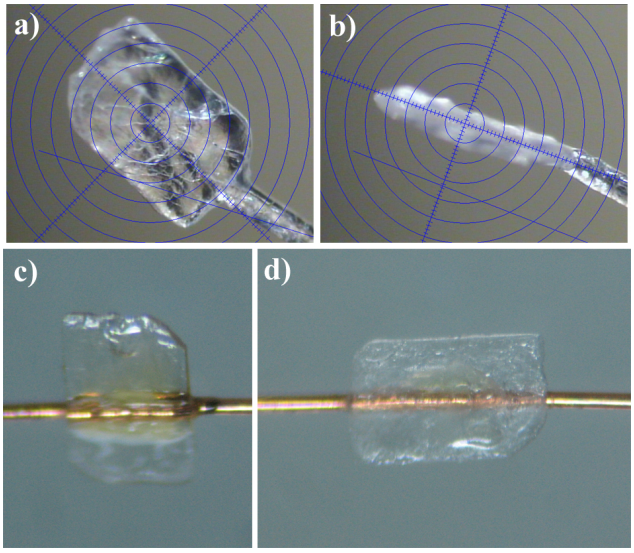


**Fig. S4** The orientated-single-crystal sample of **2** used in the magnetization measurement: a, b) the photos on the diffractmeter; c, d) the *c* axis is parallel and perpendicular to the copper wire, respectively.

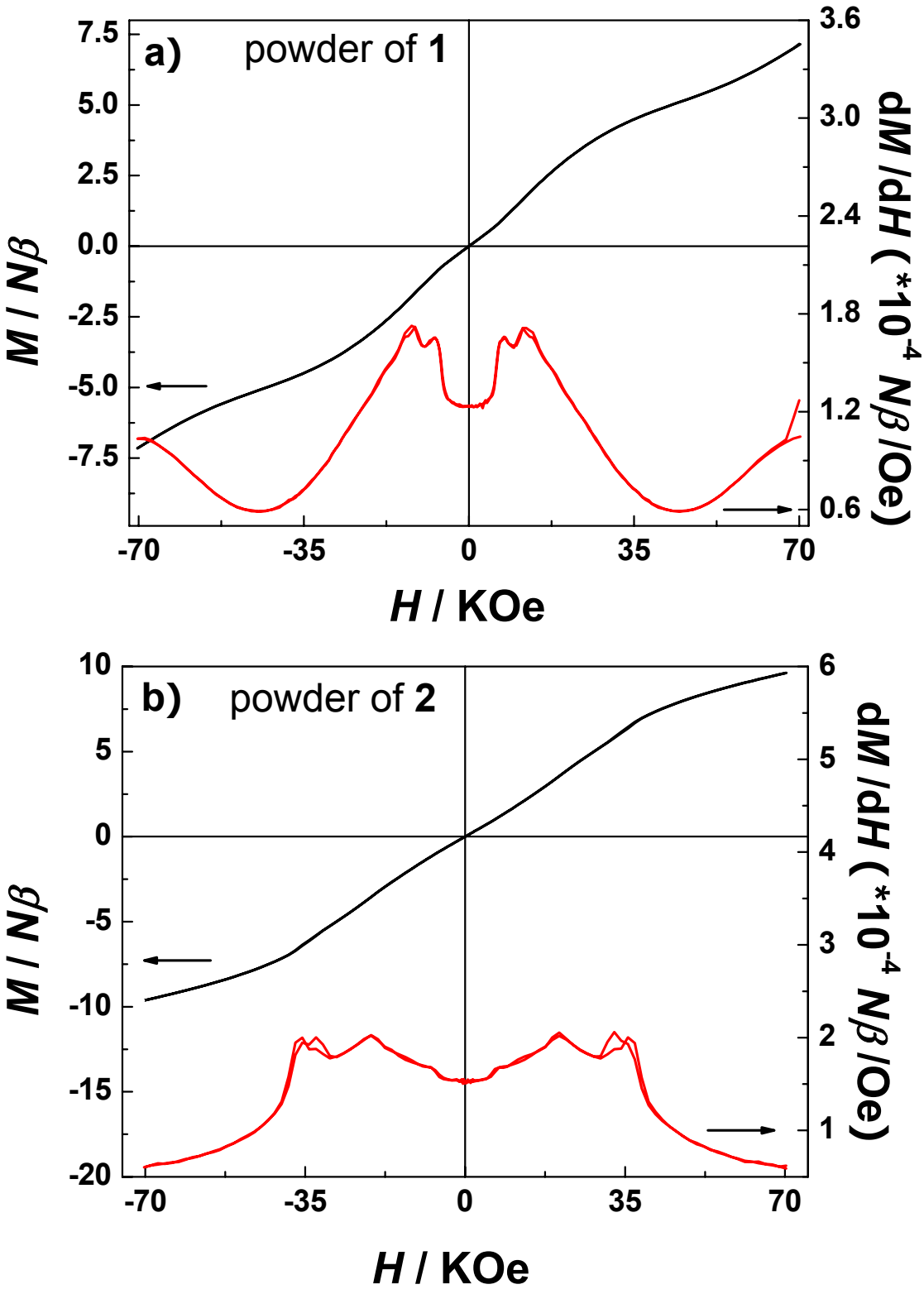


**Fig. S5** The powder magnetization (*M*) *vs*. field (*H*) hysteresis loops and their derivatives of **1** (a) and **2** (b).

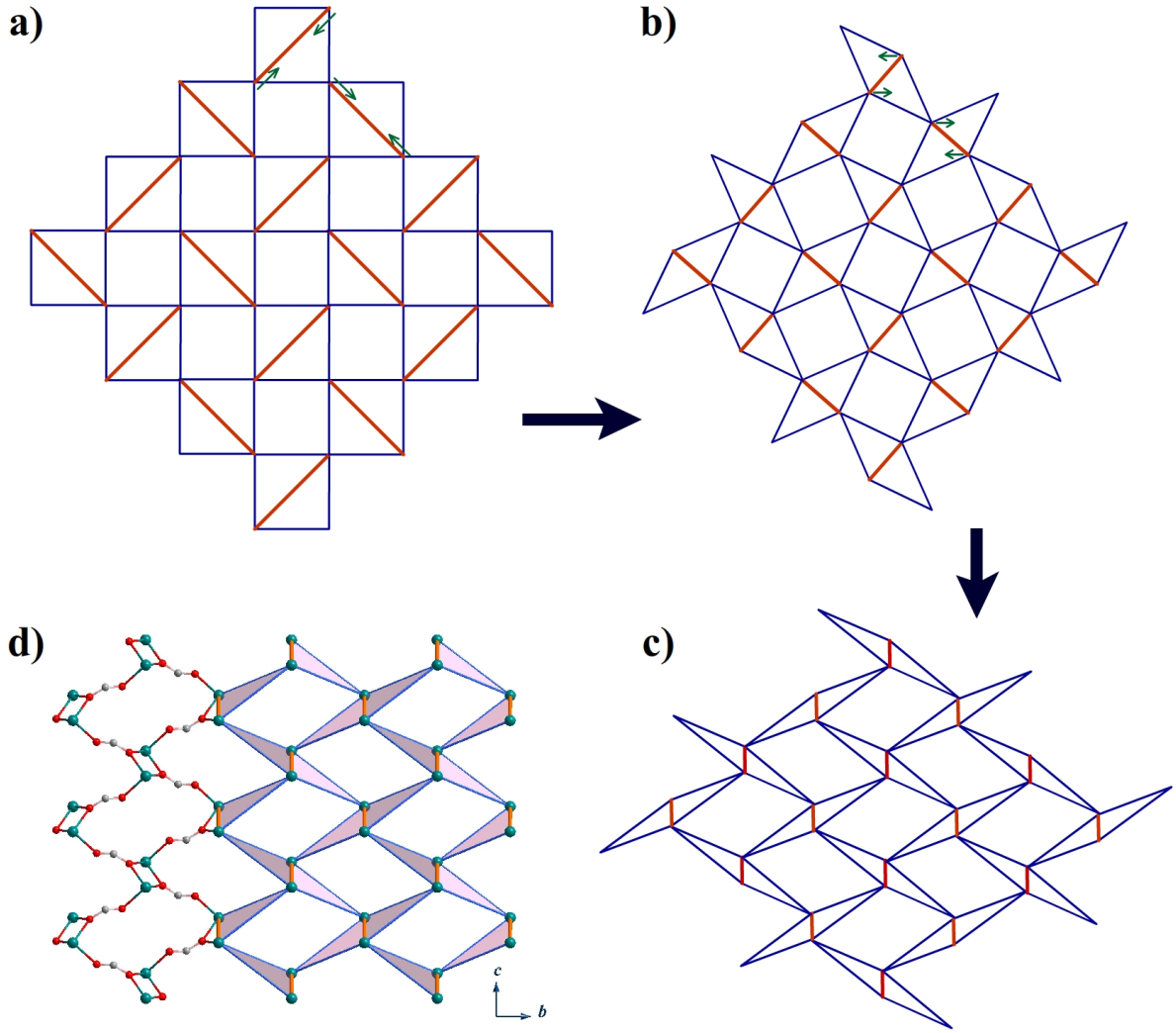


**Fig. S6** The transformation from the regular Shastry-Sutherland lattice (a) to the distorted Shastry-Sutherland lattice (c) of the planar layer in **1** (d).